

CRATERING IN GLASSES IMPACTED BY DEBRIS OR MICROMETEORITES

David E. Wiedlocher and Donald L. Kinser
Department of Materials Science and Engineering
Vanderbilt University
Nashville, TN 37235

ABSTRACT

Mechanical strength measurements on five glasses and one glass-ceramic exposed on LDEF revealed no damage exceeding experimental limits of error. The measurement technique subjected less than 5% of the sample surface area to stresses above 90% of the failure strength. Seven micrometeorite or space debris impacts occurred at locations which were not in that portion of the sample subjected to greater than 90% of the applied stress. In consequence of this the impact events on the sample were not detected in the mechanical strength measurements. The physical form and structure of the impact sites has been carefully examined to determine the influence of those events upon stress concentration associated with the impact and the resulting mechanical strength. The size of the impact site insofar as it determines flaw size for fracture purposes was examined. Surface topography of the impacts reveals that six of the seven sites display impact melting. The classical melt crater structure is surrounded by a zone of fractured glass. Residual stresses arising from shock compression and from cooling of the fused zone cannot be included in fracture mechanics analyses based on simple flaw size measurements. Strategies for refining estimates of mechanical strength degradation by impact events are presented.

INTRODUCTION

Damage of glass in space systems by space debris and micrometeorites is of interest due to the susceptibility of glass to catastrophic fracture under impact load. The Gemini window impact¹ and simulated meteoroid² impact failures in orbiter windows indicate possible catastrophic effects of impact events in space. Lunar soil samples³ collected during the Apollo 11 mission reveal micrometeorite impacts in glass spheres formed from the ejecta of larger meteorite impacts. Impacts in such glasses exhibit central melt regions surrounded by fracture zones and spall areas. These features are characteristic of many of the impacts observed on LDEF glasses. The influence of debris or micrometeorite impacts on mechanical properties of glass determine, in part, their sensitivity to the space environment.

Physical properties of six LDEF glass types listed in Table 1 were found to be unchanged by the 5.8 year exposure to low Earth-orbit⁴. The strength of exposed glasses is statistically indistinguishable from control samples as shown in Table 1. Mechanical damage to these samples included 7 impacts in the glass and glass-ceramic. The impacts had no effect on the strength reported by Wiedlocher et al⁴ due to the mechanical testing technique.

Clearly damage from the impact event will reduce the stress to induce fracture but the testing conducted did not characterize the resulting strength loss. Fracture mechanics provides a qualitative estimate of the damage induced by micrometeorite and space debris impacts.

EXPERIMENTAL PROCEDURE

The shape and size of micrometeorite and space debris damaged areas were characterized using scanning electron microscopy and stereo techniques. Fragments from the mechanical testing⁴ which contained micrometeorite or space debris impacts were gold coated and examined in an Hitachi X-650 scanning electron microscope (SEM) with ultimate resolution of approximately 5.0 nm. Stereomicrographs of each crater were taken at several magnifications and examined in stereo.

Mechanical testing of glasses impacted by micrometeorites was performed using a diametral flexure test (ASTM 394-74T) as described in reference 4. The test subjects a centrally loaded disk, supported at three points, to dynamic loading in a controlled environment. This method of testing eliminates effects of flaws on the periphery of the sample.

RESULTS

Four impacts occurred in glass samples and three occurred in glass-ceramic samples located on the trailing-edge of the satellite. Scanning electron microscopy revealed 6 of the 7 impacts contained a central crater lined with melted glass as illustrated by one of the three impacts in Zerodur shown in Figure 1. The central pit is surrounded by a zone of fragmented material with numerous radial cracks extending into the sample. The annular region adjacent to the melt zone is missing numerous fragments which spalled and were generally lost. Remnants of debris, presumed to originate from the fragmented area, were captured in the melt zone in this sample and several others. The region away from the impact site also displays damage from grit blasting with silicon carbide which was part of the sample preparation previously described⁴.

Damage surrounding the impacts extends to a radius about 5 times the central pit radius as seen in the micrograph of an impact site in Pyrex shown in Figure 2. Pre-flight sample preparation damage, not due to micrometeorite or space debris impact, is also apparent in this micrograph. Bubbles escaping the melt region of a BK-7^a sample shown in Figure 3 indicate temperatures and pressures at impact reached those needed for vaporization of the micrometeorite and/or glass. Evidence of vaporization was observed in BK-7 and soda-lime-

^aThe BK-7 glass and Zerodur glass ceramic manufactured by Schott Glass Company are identified only for reference purposes and no product endorsement is intended.

silica^b glasses which contain volatile components. Impact features in fused silica include glass fibers which extend from the melt crater as a consequence of molten glass jetting as shown in Figure 4. Fibers as long as 100 μm were observed projecting from the fused zone. One of the three impacts observed in Zerodur^a shows no evidence of melting as shown in Figure 5. Careful study of this sample at higher magnifications reveals fragmentation down to dimensions of the order of 0.5 μm . The damage associated with this impact is similar to that of impacts displaying melting except in the central fusion zone. Radially unsymmetric splash in the ejecta field of the Pyrex^c sample visible in Figure 6 indicates the micrometeorite may have impacted at an oblique angle. The crater appears to be nearly circular; however, the splash produced by the impact is strongly directional.

Mechanical stresses imposed on the tensile surface of the sample during mechanical testing are symmetric with respect to the loading points of the fixture as shown in Figure 7. Impacts not occurring in the geometrical center of the sample are subjected to stresses less than the maximum applied stress. No micrometeorite or space debris impacts occurred in the geometrical center of the samples and no fracture was observed to initiate from surface flaws associated with micrometeorite or space debris impacts. Strengths of the samples given in Table 1 include the percentage of maximum stress at the impact site determined from its location in the stress field.

DISCUSSION

One of the important questions of this work was the mass and velocity of the particles which produced the impact damage. The lower limit of velocity of particles impacting samples located on the trailing edge must be the 8 km/s orbital velocity of the satellite. The *relative* velocity required to produce the fusion zones observed in 6 of 7 cases must have been of the order of 10 km/sec based upon hyper-velocity impact tests⁵ which suggest a lower limit exists at which melting occurs in glass. Particle impacts resulting in melting generally require speeds on the order of 10 km/s although melted material has been reported at velocities as low as 6 km/s⁶. The mean impact velocities of micrometeorites and space debris impacting LDEF on row 2 has been calculated by Zook to be approximately 13 km/s⁷. We thus argue that melting in impacted glasses on the trailing edge indicates the impacts occurred with particle velocities on the order of 10 km/sec or greater. The remaining impact occurred from a particle with a velocity less than 10 km/s.

During impact ejecta with the highest velocity are generated closest to the central pit. According to the model after Melosh⁵ a particle impacting at a velocity of 13 km/s produces ejecta with velocities up to 5 km/s. Presuming fibers were produced by the highest velocity

^bThe soda-lime-silica glass manufactured by American Saint Gobain is identified only for reference purposes and no product endorsement is intended.

^cThe Pyrex glass manufactured by Corning Glass Works is identified only for reference purposes and no product endorsement is intended.

ejecta, the time to pull fibers 100 microns in length was about 2×10^{-8} seconds.

The bubbles observed in surfaces of BK-7 and soda-lime-silica glasses clearly indicate that these samples suffered pressure/temperature conditions in which boiling occurred. These phenomena may be a consequence of the energy delivery to these samples being higher than other samples or may be a consequence of the relative volatility of these two glasses. These two glasses are clearly the most volatile of those glasses examined in that they include relatively low boiling components unlike the Pyrex or fused silica glasses which did not display evidence of bubble evolution.

The highest stress at an impact site was 50% of the stress to produce failure, thus we argue that the effect of micrometeorite or space debris impacts reduced the glass strength by less than 50% for the impacts experienced in these experiments. Apart from the crater visible on the surface, damage to glass extends beneath the flaw a distance depending on propagation of the radial cracks. Though a micrometeorite impact may not penetrate the glass, the resulting defect lowers the maximum stress the glass is capable of sustaining before fracture. Stress concentration developed by the presence of a surface impact degrades the strength with a square root dependence on flaw size. Fracture mechanics⁸ permit calculation of strength from flaw size and fracture toughness parameters:

$$K_{IC} = 1.12 \sigma \sqrt{\pi \alpha}$$

where 1.12 is the free surface correction factor, σ is failure strength, and α is the flaw size. K_{IC} for Zerodur is $.9 \text{ MPam}^{1/2}$.⁹ Using a strength of 129 MPa from Table 1, the mean flaw size at the initiation site for the glass-ceramic is of the order of $10 \mu\text{m}$. Assuming the damage field from a micrometeorite or space debris impact is hemispherical, the influence of impact damage penetrating to a depth of $100 \mu\text{m}$ ($2\alpha = D$) decreases the strength to 35% of the measured value. Based on these arguments failure of the Zerodur sample should have initiated at the impact site with an applied load at the geometric center of the sample of less than 100 MPa. This suggests the extent of damage below the impact is actually no greater than 1/4 the radius of the crater observed on the surface, thus a hemispherical damage zone surrounding the impact site is improbable. This agrees with geological cratering observations which have determined the penetration depth to diameter ratio of meteorite impacts in the Earth's strata to be about 1/3 to 1/4. Deviations of the depth/diameter ratio from 1/3 arise from changing physical properties of the projectile and target.

Cratering mechanics⁵ indicate that typical projectile diameters are 1/3 the central pit diameter which gives a projectile size between $15 \mu\text{m}$ and $30 \mu\text{m}$ for most impacts observed here. Some ambiguity in crater dimension measurement occurs with our measurements. The literature often discusses impacts in soils or metals and the diameter measured at the lip of the uplifted zone is commonly used. In our case the central melt crater whose dimensions are easily characterized and the extrema of the radial cracks could easily be measured but no uplifted zone has been identified, hence the use of the term "crater diameter" is potentially ambiguous when applied to our work.

Crater shape is relatively independent⁵ of impact angle for impacts at angles greater than

10° from the surface plane of the target. Projectile shape largely determines crater shape, even for normal impact. Impact features believed to arise from meteorites incident at angles between 20° and 45° have been observed in lunar craters⁵. The unsymmetric glass ejecta or debris field associated with the impact in the Pyrex sample is evidence that impact occurred at an oblique angle. As previously discussed, the formation of frozen strands of glass develops in the early stages of impact. This would account for the extension of filaments in the direction of impact before excavation of the crater was complete. Also, radial cracks extending from the impact extrapolate to an origin off center of the excavation in the direction of the splash. These observations indicate the projectile velocity had a large component in the direction of the debris field.

CONCLUSIONS

1. Six of the seven impact events on glass and glass ceramic samples exposed on LDEF produced melting or vaporization in craters which are similar to those produced by laboratory impacts at velocities above 10 km/s.
2. Glass fibers produced during impact by jetting of molten material have been observed with lengths up to approximately 100 μm . Presuming that these fibers were produced from ejecta with maximum velocity, the fibers were produced in about 2×10^{-8} second.
3. The impact observed in Pyrex may have occurred at an oblique angle.
4. The damage field associated with the 7 impact features cannot be treated as hemispherical. Flaw size determined from the depth of penetration scales similar to geological depth to diameter ratios. This depth is on the order of 1/5 the crater diameter. Based on this flaw size the mechanical strength after the impact event is approximately 1/2 of the original.

ACKNOWLEDGEMENTS

The authors gratefully acknowledge financial support of NASA through grants NAS-8-156 and NAS-8-32695 and contract L-17761D.

Table 1
Mechanical Strength and Impact Site Damage Size

Sample	Strength (MPa)	Standard Deviation (MPa)	Strength Control (MPa)	Standard Deviation (MPa)	Stress Contour (% Max)	Central Melt Pit Diameter μm	Crater Diameter μm	Spall Surface Diameter μm
BK-7	126	8	124	8	10	40	100	200
Fused Silica	97	4	97	4	38	50	120	250
Soda-lime-silica	104	4	100	9	35	80	175	475
Pyrex	105	7	111	4	10	85	200	400
Vycor	101	5	103	4	NI ^d	NI	NI	NI
Zerodur (I) ^e	129	8	128	5	30	NM ^f	100	275
Zerodur (II)	129	8	128	5	50	75	200	400
Zerodur (III)	129	8	128	5	25	50	150	300

^dNI indicates no impact on this type sample.

^eThe mechanical strength reported is the average of a group of 9 samples while impacts were measured on three individual samples.

^fNo melt zone observed.

REFERENCES

1. J. B. Singletary and J. B. Rittenhouse, "Spacecraft Materials Experience," *Space Materials Handbook*, 3rd ed., NASA SP-3051, 1969.
2. J. W. Gehring, Jr., "Engineering Considerations in Hyper-velocity Impact," Chapter IX in *High-Velocity Impact Phenomena*, edited by R. Kinslow Academic Press, NY, 1970.
3. C. Frondel, C. Klein, J. Ito and J. C. Drake, "Mineralogical and Chemical Studies of Apollo 11 Lunar Fines and Selected Rocks," *Proceedings of the Apollo 11 Lunar Science Conference*, Vol. 1, Pergamon Press, New York, 445-474, 1970.
4. D. E. Wiedlocher, D. L. Kinser, D. S. Tucker and R. Nichols, "Low Earth-Orbit Effects on Strength of Glasses," *J. Am. Cer. Soc.*, Vol. 75, Nov. 1992.
5. H. J. Melosh, *Impact Cratering: A Geological Process*, Oxford Monographs on Geology and Geophysics No. 11, Oxford University Press, New York, 1989.
6. D. E. Gault, cited by H. J. Melosh, *ibid.*
7. H. A. Zook, "Meteoroid Directionality on LDEF and Asteroidal versus Cometary Sources," *Lunar Planet. Sci. XXII*, 1577-1578, 1991.
8. S. W. Freiman, "Fracture Mechanics of Glass," *Glass: Science and Technology*, Vol. 5, *Elasticity and Strength in Glasses*, ed. by D. R. Uhlmann and N. J. Kreidl, Academic Press, New York, 1980.
9. M. J. Viens, "Fracture Toughness and Crack Growth of Zerodur," NASA Technical Memorandum 4185, NASA Scientific and Technical Information Division, 1990.

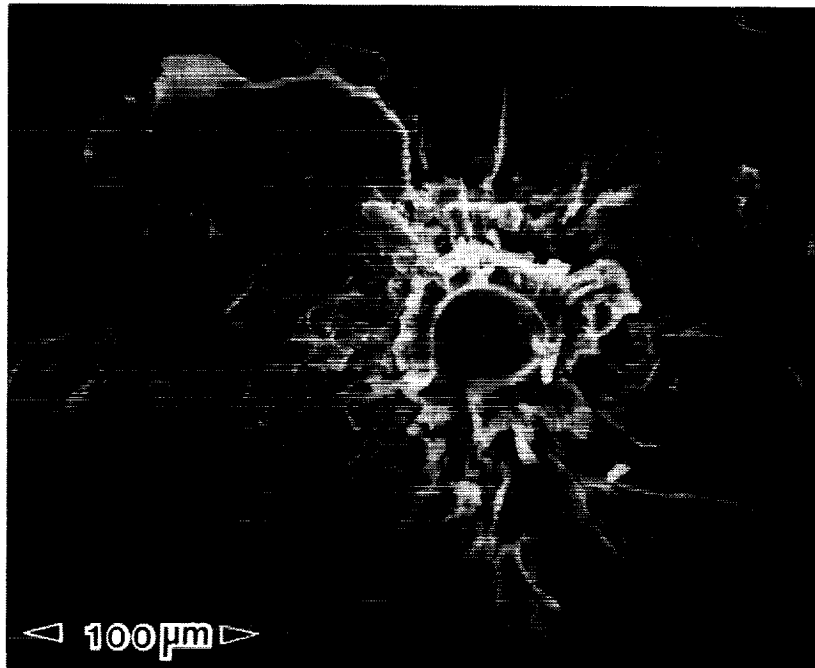


Figure 1: Scanning electron micrograph of impact in Zerodur displaying melt crater formation.



Figure 2: Scanning electron micrograph of impact crater in Pyrex displaying impact melting.

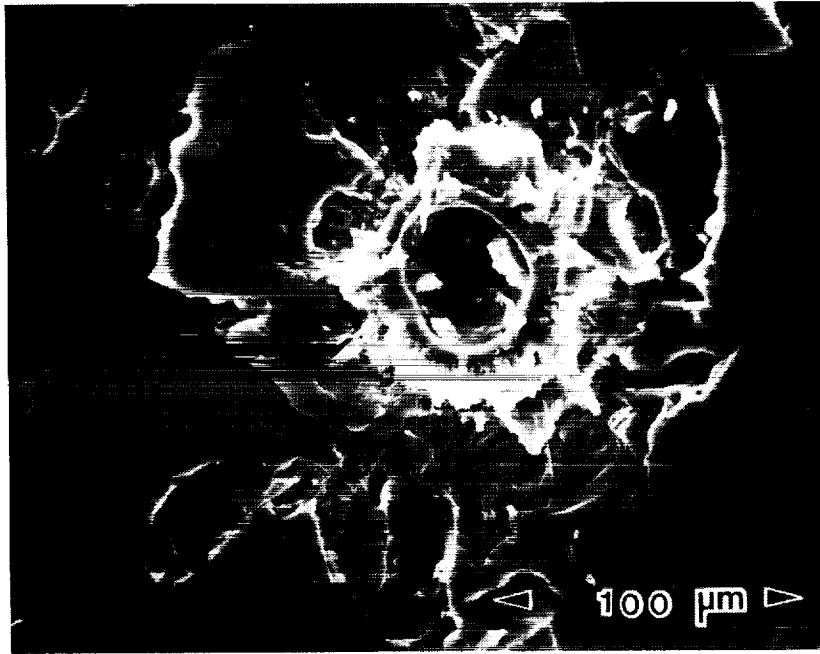


Figure 3: Scanning electron micrograph of impact crater in BK-7 glass displaying melt zone and trapped bubbles.

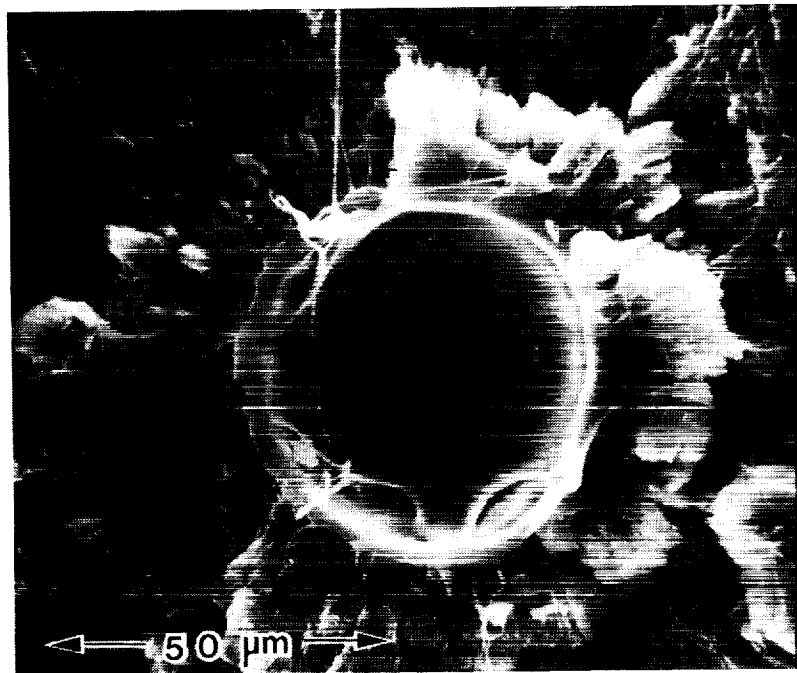


Figure 4: Scanning electron micrograph of impact crater in fused silica glass displaying jetting of molten glass and resulting glass fibers extending from melt crater.

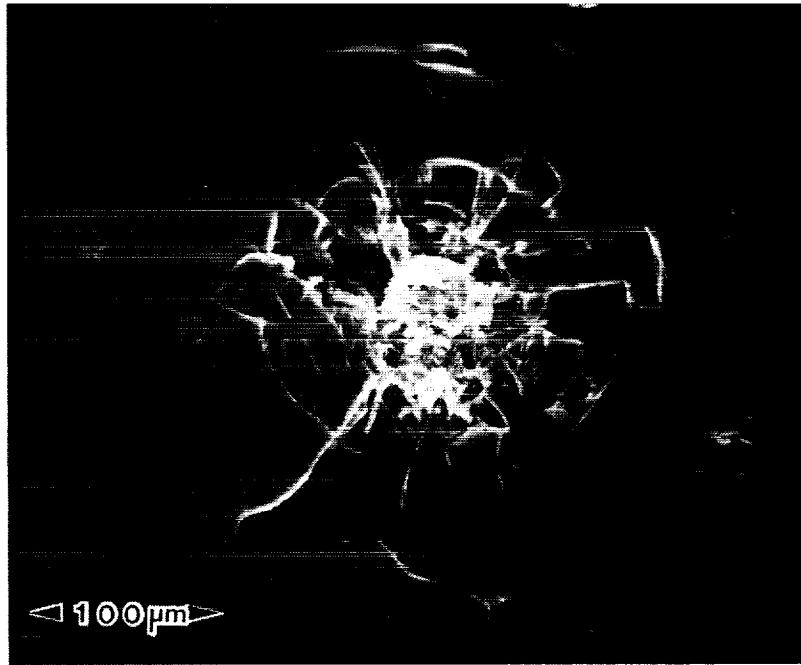


Figure 5: Scanning electron micrograph of impact site in Zerodur which displays no evidence of impact fusion.

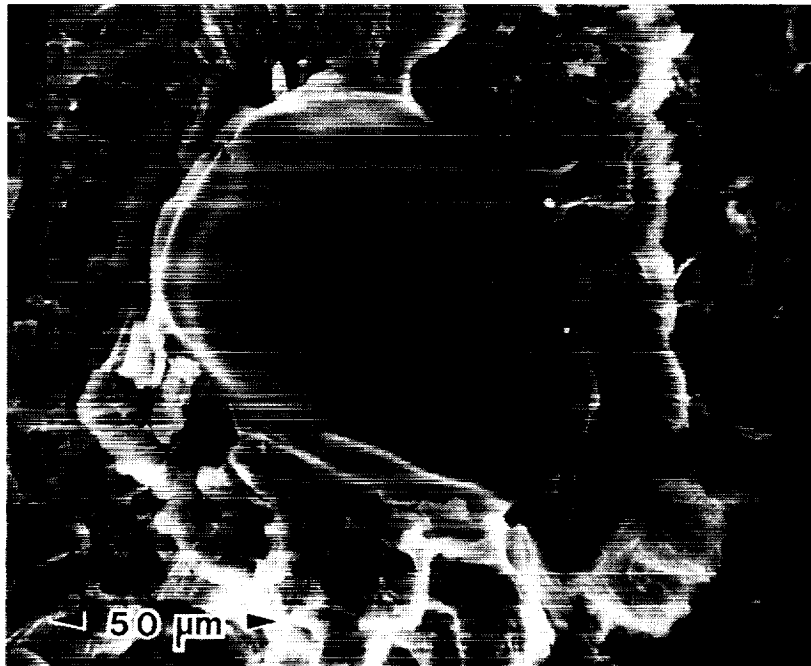


Figure 6: Scanning electron micrograph of impact crater in Pyrex displaying unsymmetric splash of ejecta possibly arising from oblique impact.

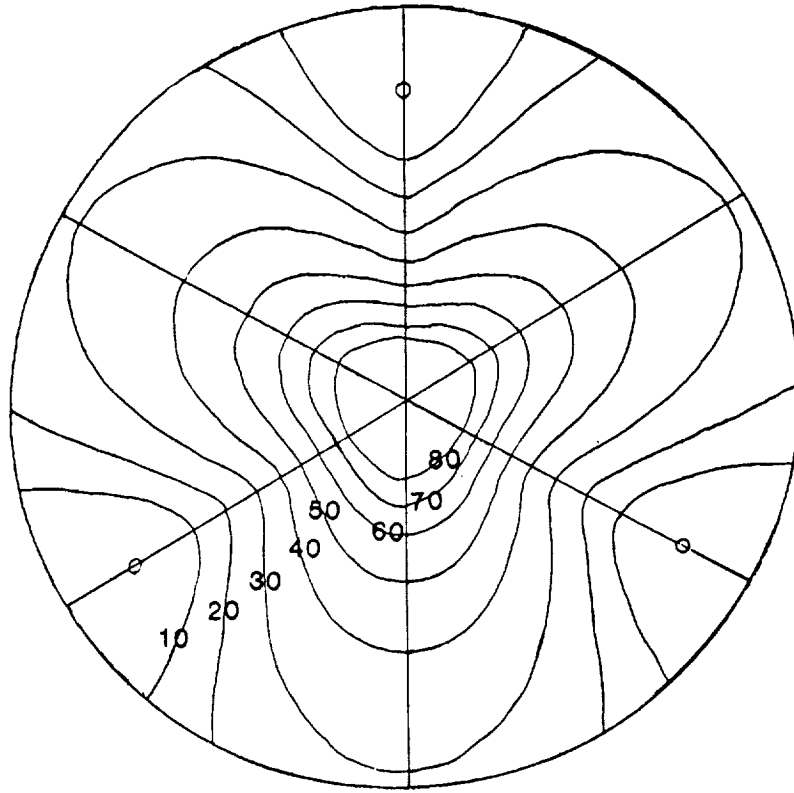


Figure 7: Stress contour diagram for mechanical testing employing three point support with central load.

